Hermite and spline interpolation algorithms for planar & spatial Pythagorean-hodograph curves

Rida T. Farouki

Department of Mechanical & Aeronautical Engineering,
University of California, Davis

— synopsis —

- motivation for Hermite & spline interpolation algorithms
- planar PH quintic Hermite interpolants (four solutions)
- computing absolute rotation index & elastic bending energy
- a priori identification of “good” Hermite interpolant
- planar C^2 PH quintic splines — numerical methods
- spatial PH quintic Hermite interpolants (2 free parameters)
- spatial PH quintics — taxonomy of special types
- spatial C^2 PH quintic splines — residual freedoms

motivation for Hermite & spline interpolation algorithms

- only cubic PH curves characterizable by simple constraints on Bézier control polygons

- planar PH cubics $=$ Tschirnhausen's cubic,
  spatial PH cubics $= \{$ helical cubic space curves $\}$
  — too limited for general free–form design applications

- construct quintic PH curves "geometrically" by interpolation of discrete data — points, tangents, etc.

- non–linear interpolation equations made tractable by complex number model for planar PH curves, and quaternion or Hopf map model for spatial PH curves

- efficient algorithms allow interactive design of PH curves

Pythagorean triples of polynomials

$$x'^2(t) + y'^2(t) = \sigma^2(t) \qquad \Longleftrightarrow \qquad \begin{cases} x'(t) = u^2(t) - v^2(t) \\ y'(t) = 2\,u(t)v(t) \\ \sigma(t) = u^2(t) + v^2(t) \end{cases}$$

K. K. Kubota, Pythagorean triples in unique factorization domains, *American Mathematical Monthly* **79**, 503–505 (1972)

R. T. Farouki and T. Sakkalis, Pythagorean hodographs, *IBM Journal of Research and Development* **34** 736–752 (1990)

R. T. Farouki, The conformal map $z \to z^2$ of the hodograph plane, *Computer Aided Geometric Design* **11**, 363–390 (1994)

complex number model for planar PH curves

choose complex polynomial $\mathbf{w}(t) = u(t) + \mathrm{i}\,v(t)$

$\longrightarrow$ planar Pythagorean hodograph $\mathbf{r}'(t) = (x'(t), y'(t)) = \mathbf{w}^2(t)$

planar PH quintic Hermite interpolants

R. T. Farouki and C. A. Neff, Hermite interpolation by Pythagorean–hodograph quintics, *Mathematics of Computation* **64**, 1589–1609 (1995)

complex representation: hodograph $=$ [complex quadratic polynomial]^2

$$\mathbf{r}'(t) \;=\; [\,\mathbf{w}_0(1-t)^2 + \mathbf{w}_1 2(1-t)t + \mathbf{w}_2 t^2\,]^{\,2}$$

$$\mathbf{r}(t) \;=\; \int \mathbf{r}'(t)\;\mathrm{d}t \;=\; \sum_{k=0}^{5} \mathbf{p}_k \binom{5}{k} (1-t)^{5-k} t^k$$

complex Hermite data — $\mathbf{r}'(0) = \mathbf{d}_0,\;\; \mathbf{r}'(1) = \mathbf{d}_1,\;\; \mathbf{r}(1) - \mathbf{r}(0) = \Delta\mathbf{p}$

$\rightarrow$ three quadratic equations in three complex variables $\mathbf{w}_0,\, \mathbf{w}_1,\, \mathbf{w}_2$

$$\mathbf{w}_0^2 = \mathbf{d}_0\,, \quad \mathbf{w}_2^2 = \mathbf{d}_1\,, \quad \mathbf{w}_0^2 + \mathbf{w}_0\mathbf{w}_1 + \frac{2\mathbf{w}_1^2 + \mathbf{w}_2\mathbf{w}_0}{3} + \mathbf{w}_1\mathbf{w}_2 + \mathbf{w}_2^2 = 5\Delta\mathbf{p}$$

generically four distinct interpolants to given Hermite data $\mathbf{d}_0$, $\mathbf{d}_1$, $\Delta\mathbf{p}$

one good solution among four PH quintic interpolants —
other three typically exhibit undesired “looping” behavior

obtain Bézier control points of PH quintic from $\mathbf{w}_0$, $\mathbf{w}_1$, $\mathbf{w}_2$

$$\begin{aligned}
\mathbf{p}_1 &= \mathbf{p}_0 + \frac{\mathbf{w}_0^2}{5}\,, \\
\mathbf{p}_2 &= \mathbf{p}_1 + \frac{\mathbf{w}_0\mathbf{w}_1}{5}\,, \\
\mathbf{p}_3 &= \mathbf{p}_2 + \frac{2\mathbf{w}_1^2 + \mathbf{w}_0\mathbf{w}_2}{15}\,, \\
\mathbf{p}_4 &= \mathbf{p}_3 + \frac{\mathbf{w}_1\mathbf{w}_2}{5}\,, \\
\mathbf{p}_5 &= \mathbf{p}_4 + \frac{\mathbf{w}_2^2}{5}\,.
\end{aligned}$$

four distinct PH quintic Hermite interpolants

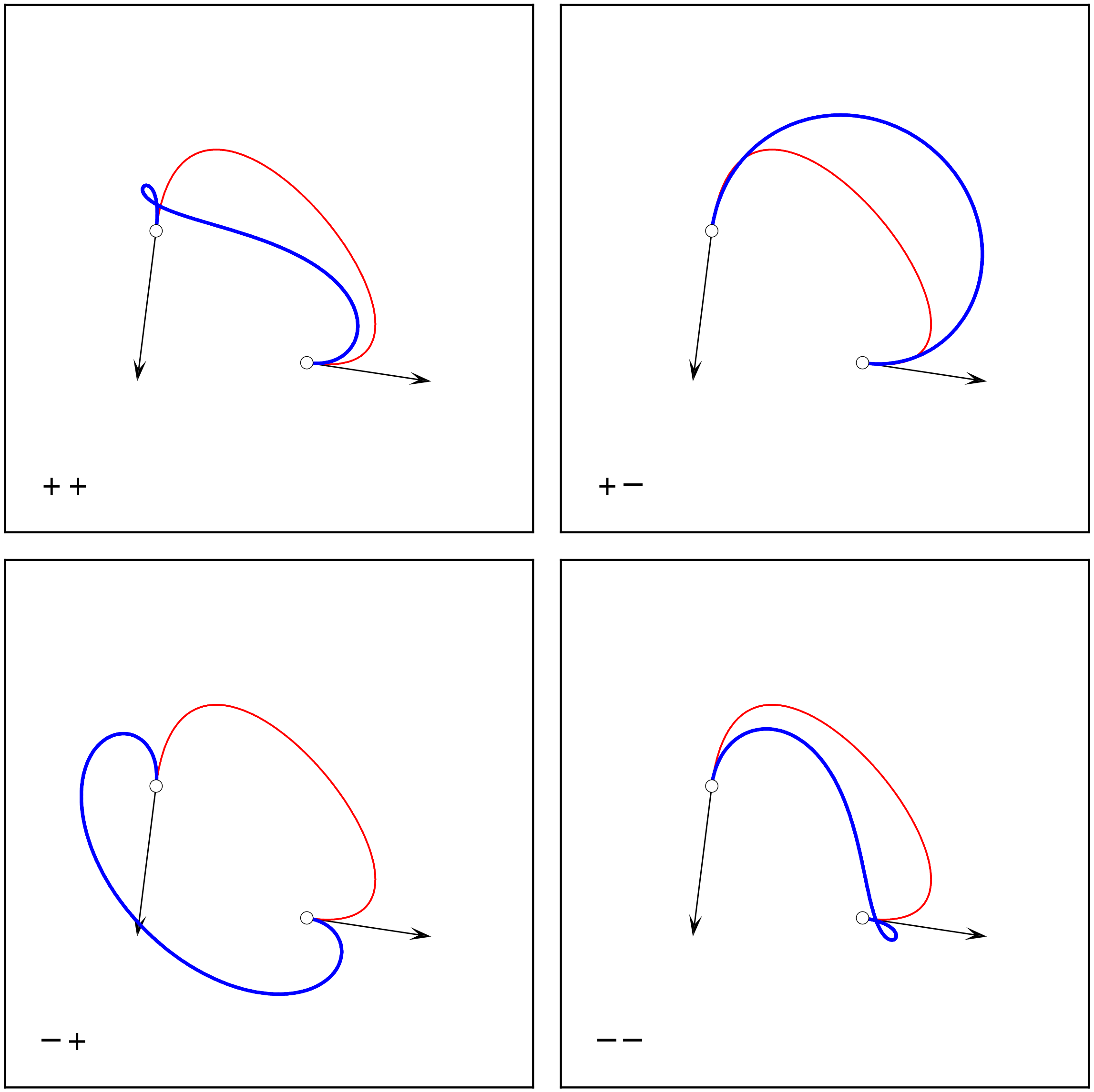

blue = PH quintic, red = "ordinary" cubic

choosing the "good" interpolant — rotation index

absolute rotation index: $$R_{\rm abs} \;=\; \frac{1}{2\pi}\int |\kappa|\,\mathrm{d}s$$

w.l.o.g. take $\mathbf{r}(0)=0$ and $\mathbf{r}(1)=1$ (shift + scale of Hermite data)

$$\mathbf{r}'(t) \;=\; \mathbf{k}\,[\,(t-\mathbf{a})(t-\mathbf{b})\,]^2$$

solve for $\mathbf{k}$, $\mathbf{a}$, $\mathbf{b}$ instead of $\mathbf{w}_0$, $\mathbf{w}_1$, $\mathbf{w}_2$

locations of $\mathbf{a}$, $\mathbf{b}$ relative to $[\,0,1\,]$ gives $R_{\rm abs}$:

$$R_{\rm abs} \;=\; \frac{\angle\,0\,\mathbf{a}\,1 \;+\; \angle\,0\,\mathbf{b}\,1}{\pi} \quad \text{(no inflections)}$$

$$R_{\rm abs} \;=\; \frac{1}{\pi}\sum_{k=0}^{N}\,|\,\angle\,t_k\,\mathbf{a}\,t_{k+1} \;-\; \angle\,t_k\,\mathbf{b}\,t_{k+1}\,|$$

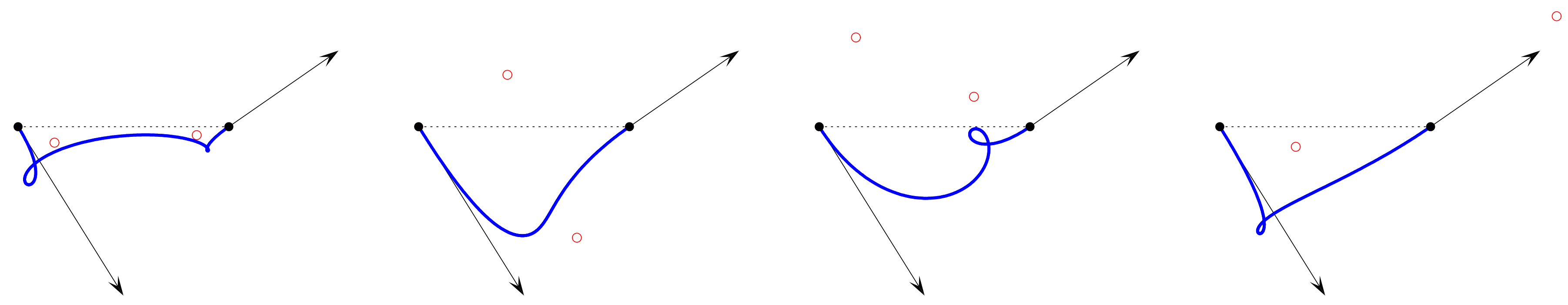

Computation of absolute rotation index $R_{\rm abs}$ from locations of the complex hodograph roots $\mathbf{a}$, $\mathbf{b}$ relative to $t \in [\,0,1\,]$. The best interpolant arises when $\mathbf{a}$, $\mathbf{b}$ lie on opposite sides of (and are not close to) this interval.

choosing the "good" interpolant — bending energy

$$U \;=\; \int \kappa^2 \, \mathrm{d}s \;=\; \int \frac{|\mathbf{r}' \times \mathbf{r}''|^2}{\sigma^5} \, \mathrm{d}t$$

use complex form $\mathbf{r}'(t) = \mathbf{w}^2(t)$ with $\mathbf{w}(t) = \mathbf{k}(t-\mathbf{a})(t-\mathbf{b})$ again

analytic reduction of indefinite integral

$$\begin{aligned} U(t) \;=\; \frac{4}{|\mathbf{k}|^2} \bigg\{ & \, 2\,\mathrm{Re}(\mathbf{a}_1)\ln|t-\mathbf{a}| \;+\; 2\,\mathrm{Re}(\mathbf{b}_1)\ln|t-\mathbf{b}| \\ & - 2\,\mathrm{Im}(\mathbf{a}_1)\arg(t-\mathbf{a}) \;-\; 2\,\mathrm{Im}(\mathbf{b}_1)\arg(t-\mathbf{b}) \\ & - \mathrm{Re}\left[\frac{2\,\mathbf{a}_2}{t-\mathbf{a}} + \frac{2\,\mathbf{b}_2}{t-\mathbf{b}} + \frac{\mathbf{a}_3}{(t-\mathbf{a})^2} + \frac{\mathbf{b}_3}{(t-\mathbf{b})^2} \right] \bigg\} \,. \end{aligned}$$

$\mathbf{a}_1, \mathbf{b}_1, \mathbf{a}_2, \mathbf{b}_2, \mathbf{a}_3, \mathbf{b}_3 =$ coefficients in partial fraction expansion of integrand

total bending energy of PH quintic $E = U(1) - U(0)$

compare PH quintic & “ordinary” cubic interpolants

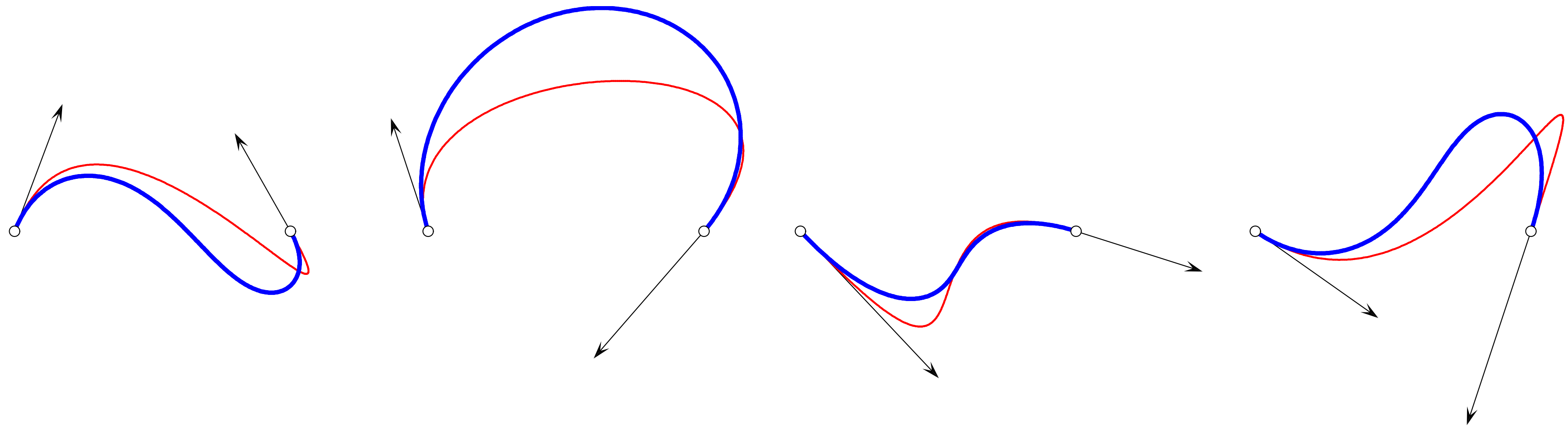

good PH quintic interpolants (blue) to first-order Hermite data typically have lower bending energy than “ordinary” cubic interpolants (red)

C^2 spatial Hermite interpolants:

B. Jüttler, C^2 Hermite interpolation by Pythagorean hodograph curves of degree seven, *Mathematics of Computation* **70**, 1089–1111 (2001)

monotone–curvature PH quintic segments

D. J. Walton and D. S. Meek, A Pythagorean–hodograph quintic spiral, *Computer Aided Design* **28**, 943–950 (1996)

R. T. Farouki, Pythagorean–hodograph quintic transition curves of monotone curvature, *Computer Aided Design* **29**, 601–606 (1997)

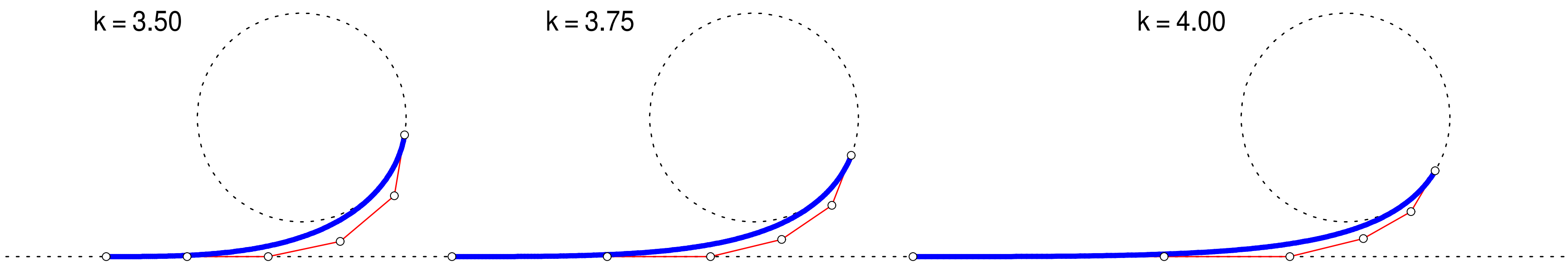

G^2 blends between a line and a circle, defined by PH quintics of monotone curvature (the Bézier control polygons of the PH quintics are also shown) — the free parameter k controls the rate of increase of the curvature.

a priori identification of “good” interpolant

H. P. Moon, R. T. Farouki, and H. I. Choi, Construction and shape analysis of PH quintic Hermite interpolants, *Computer Aided Geometric Design* **18**, 93–115 (2001)

H. I. Choi, R. T. Farouki, S. H. Kwon, and H. P. Moon, Topological criterion for selection of quintic Pythagorean–hodograph Hermite interpolants, *Computer Aided Geometric Design* **25**, 411–433 (2008)

if the end derivatives $\mathbf{d}_0, \mathbf{d}_1$ lie in complex–plane domain D defined by

$$D = \{ \, \mathbf{d} \mid \mathrm{Re}(\mathbf{d}) > 0 \text{ and } |\mathbf{d}| < 3 \, \}$$

— i.e., they point in the direction of $\Delta\mathbf{p}$ and have magnitudes commensurate with $|\Delta\mathbf{p}|$, the “good” PH quintic corresponds to the $++$ choice of signs in the solution procedure

criterion for “good” solution — absence of anti–parallel tangents relative to the “ordinary” cubic Hermite interpolant

construction of C^2 PH quintic splines versus "ordinary" C^2 cubic splines

- both incur global system of equations in three consecutive unknowns
- both require specification of end conditions to complete the equations
- equations for "ordinary" cubic splines arise from C^2 continuity condition at each interior node, while equations for PH quintic splines arise from interpolating consecutive points $\mathbf{p}_i$, $\mathbf{p}_{i+1}$
- "ordinary" cubic splines incur linear equations in real variables, but PH quintic splines incur quadratic equations in complex variables
- coordinate components of "ordinary" cubic splines weakly coupled through nodal parameter values; components of PH quintic splines strongly coupled through PH property
- linearity of "ordinary" cubic splines $\Rightarrow$ unique interpolant and spline basis methods, but non–linear nature of PH quintic splines $\Rightarrow$ multiplicity of solutions and no linear superposition

planar C^2 PH quintic spline equations

problem: construct C^2 piecewise–PH–quintic curve interpolating given sequence of points $\mathbf{p}_0, \ldots, \mathbf{p}_N \in \mathbb{R}^2$

using complex representation of planar PH quintics, write hodograph of segment $\mathbf{r}_i(t)$ between $\mathbf{p}_{i-1}$ and $\mathbf{p}_i$, as square of a complex quadratic:

$$\mathbf{r}_i'(t) \;=\; [\; \tfrac{1}{2}(\mathbf{z}_{i-1} + \mathbf{z}_i)(1-t)^2 + \mathbf{z}_i \, 2(1-t)t + \tfrac{1}{2}(\mathbf{z}_i + \mathbf{z}_{i+1})t^2 \;]^2$$

$\Rightarrow$ $\mathbf{r}_i(t)$ and $\mathbf{r}_{i+1}(t)$ automatically satisfy C^1 and C^2 conditions at their juncture $\mathbf{p}_i = \mathbf{r}_i(1) = \mathbf{r}_{i+1}(0)$ — namely,

$$\mathbf{r}_i'(1) = \mathbf{r}_{i+1}'(0) = \tfrac{1}{4}(\mathbf{z}_i + \mathbf{z}_{i+1})^2, \quad \mathbf{r}_i''(1) = \mathbf{r}_{i+1}''(0) = (\mathbf{z}_{i+1} - \mathbf{z}_i)(\mathbf{z}_i + \mathbf{z}_{i+1})$$

writing $\Delta\mathbf{p}_i = \mathbf{p}_i - \mathbf{p}_{i-1}$, the end–point interpolation condition

$$\int_0^1 \mathbf{r}_i'(t) \, \mathrm{d}t \;=\; \Delta\mathbf{p}_i$$

yields for $i = 1, \ldots, N$ the equations

$$\begin{aligned}\mathbf{f}_i(\mathbf{z}_1, \ldots, \mathbf{z}_N) \;&=\; 3\,\mathbf{z}_{i-1}^2 \;+\; 27\,\mathbf{z}_i^2 \;+\; 3\,\mathbf{z}_{i+1}^2 \;+\; \mathbf{z}_{i-1}\mathbf{z}_{i+1} \\ &\quad + \; 13\,\mathbf{z}_{i-1}\mathbf{z}_i \;+\; 13\,\mathbf{z}_i\mathbf{z}_{i+1} \;-\; 60\,\Delta\mathbf{p}_i \;=\; 0\end{aligned}$$

in the N complex variables $\mathbf{z}_1, \ldots \mathbf{z}_N$. First & last equations modified using chosen end conditions to avoid reference to undefined variables $\mathbf{z}_0, \mathbf{z}_{N+1}$.

possible choices for end conditions

- specified end derivatives — $\mathbf{r}_1'(0) = \mathbf{d}_0$ and $\mathbf{r}_N'(1) = \mathbf{d}_N$
- cubic (Tschirnhaus) end spans — $\mathbf{r}_1(t)$, $\mathbf{r}_N(t)$ are just PH cubics
- periodic end conditions — set $\mathbf{r}_N'(1) = \mathbf{r}_1'(0)$ and $\mathbf{r}_N''(1) = \mathbf{r}_1''(0)$ for a closed C^2 curve with $\mathbf{p}_N = \mathbf{p}_0$
- no analog of not–a–knot condition for “ordinary” C^2 cubic splines

solution method #1 — homotopy scheme

G. Albrecht and R. T. Farouki, Construction of C^2 Pythagorean–hodograph interpolating splines by the homotopy method , *Advances in Computational Mathematics* **5**, 417–442 (1996)

the non–linear system to be solved: $\mathbf{f}_i(\mathbf{z}_1, \ldots, \mathbf{z}_N) = 0\,, \ \ 1 \le i \le N$

“initial” system with <u>known</u> solutions: $\mathbf{g}_i(\mathbf{z}_1, \ldots, \mathbf{z}_N) = 0\,, \ \ 1 \le i \le N$

“continuously deform” initial system into desired system while tracking all solutions as homotopy parameter λ increases from 0 to 1

$$\mathbf{h}_i(\mathbf{z}_1, \ldots, \mathbf{z}_N, \lambda) \;=\; \lambda\, \mathbf{f}_i(\mathbf{z}_1, \ldots, \mathbf{z}_N) \;+\; (1-\lambda)\, \mathrm{e}^{\mathrm{i}\phi}\, \mathbf{g}_i(\mathbf{z}_1, \ldots, \mathbf{z}_N) \;=\; 0$$

2^{N+k} non-singular solution loci $(\mathbf{z}_1, \ldots, \mathbf{z}_N, \lambda) \in \mathbb{C}^N \times \mathbb{R}$ for “almost all” ϕ

predictor-corrector method

trace from $\lambda = 0$ to 1 loci defined by $\mathbf{h}_i(\mathbf{z}_1, \ldots, \mathbf{z}_N, \lambda) = 0$, $1 \leq i \leq N$

tridiagonal Jacobian matrix: $$\mathbf{M}_{ij} = \frac{\partial \mathbf{h}_i}{\partial \mathbf{z}_j}\,, \quad 1 \leq i, j \leq N$$

predictor step : motion along *tangent* directions to solution loci

$$\sum_{j=1}^{N} \mathbf{M}_{ij}\, \Delta \mathbf{z}_j = (\mathrm{e}^{\mathrm{i}\phi}\, \mathbf{g}_i - \mathbf{f}_i)\, \Delta\lambda\,, \quad i = 1, \ldots, N$$

corrector step : correct for curvature of loci by Newton iterations

$$\mathbf{z}_j^{(r+1)} = \mathbf{z}_j^{(r)} + \delta \mathbf{z}_j \qquad \text{for } j = 1, \ldots, N\,, \quad r = 1, 2, \ldots$$

where $$\sum_{j=1}^{N} \mathbf{M}_{ij}^{(r)}\, \delta \mathbf{z}_j = -\,\mathbf{h}_i^{(r)}\,, \quad i = 1, \ldots, N$$

until $$\sum_{i=1}^{N} |\, \mathbf{h}_i(\mathbf{z}_1^{(r)}, \ldots, \mathbf{z}_N^{(r)}, \lambda + \Delta\lambda)\, |^2 \leq \epsilon^2$$

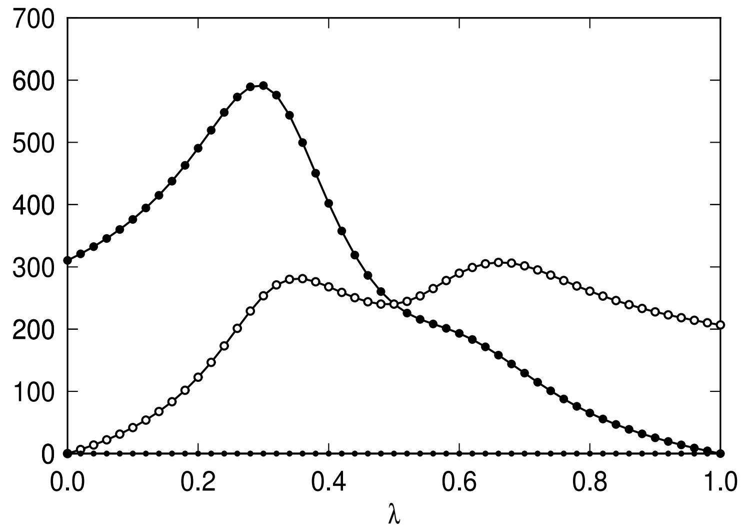

typical behavior of $\|\mathbf{f}\|_2$, $\|\mathbf{g}\|_2$, $\|\mathbf{h}\|_2$ norms in predictor–corrector scheme

- well–conditioned — accuracy near machine precision achievable

- gives complete set of 2^{N+k} distinct PH quintic spline interpolants ($k = -1, 0, +1$ depends on chosen end conditions)

- unique good interpolant — without undesired "looping" behavior

- better shape (curvature distribution) than "ordinary" C^2 cubic spline

- becomes computationally very expensive for large N

complete set of PH quintic spline interpolants

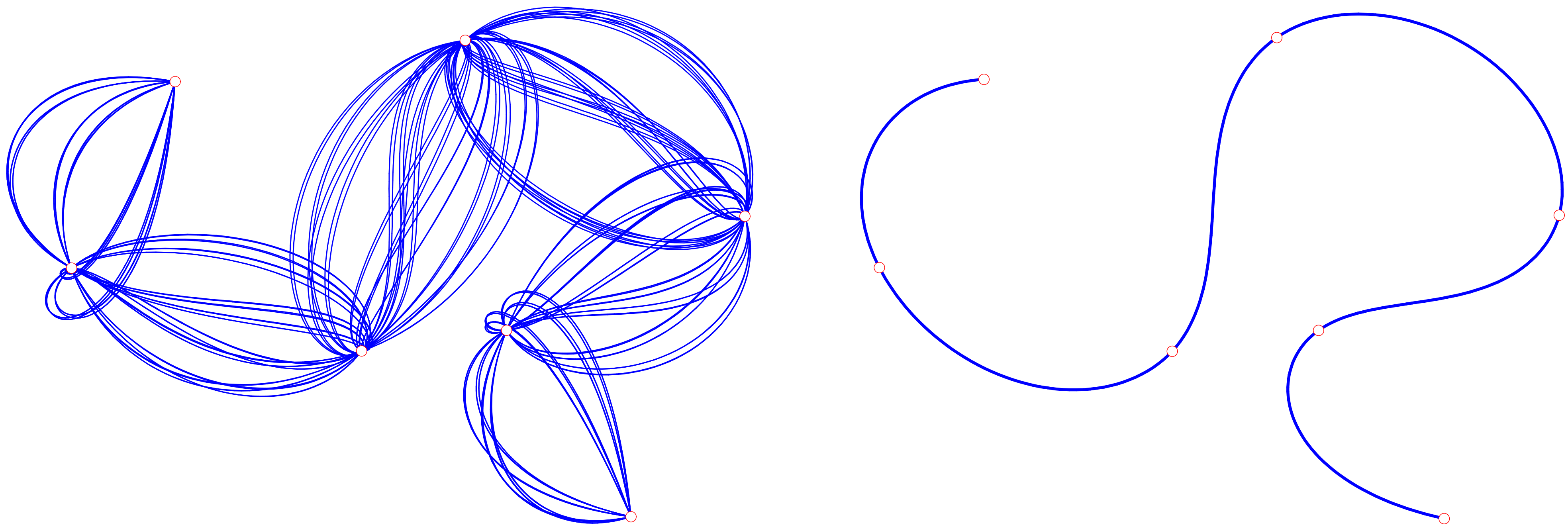

shape measures for identifying “good” interpolant:

total arc length, absolute rotation index, elastic bending energy

$$S = \int \mathrm{d}s\,, \qquad R_{\mathrm{abs}} = \frac{1}{2\pi}\int |\kappa|\,\mathrm{d}s\,, \qquad E = \int \kappa^2\,\mathrm{d}s$$

comparison of PH quintic & “ordinary” cubic splines

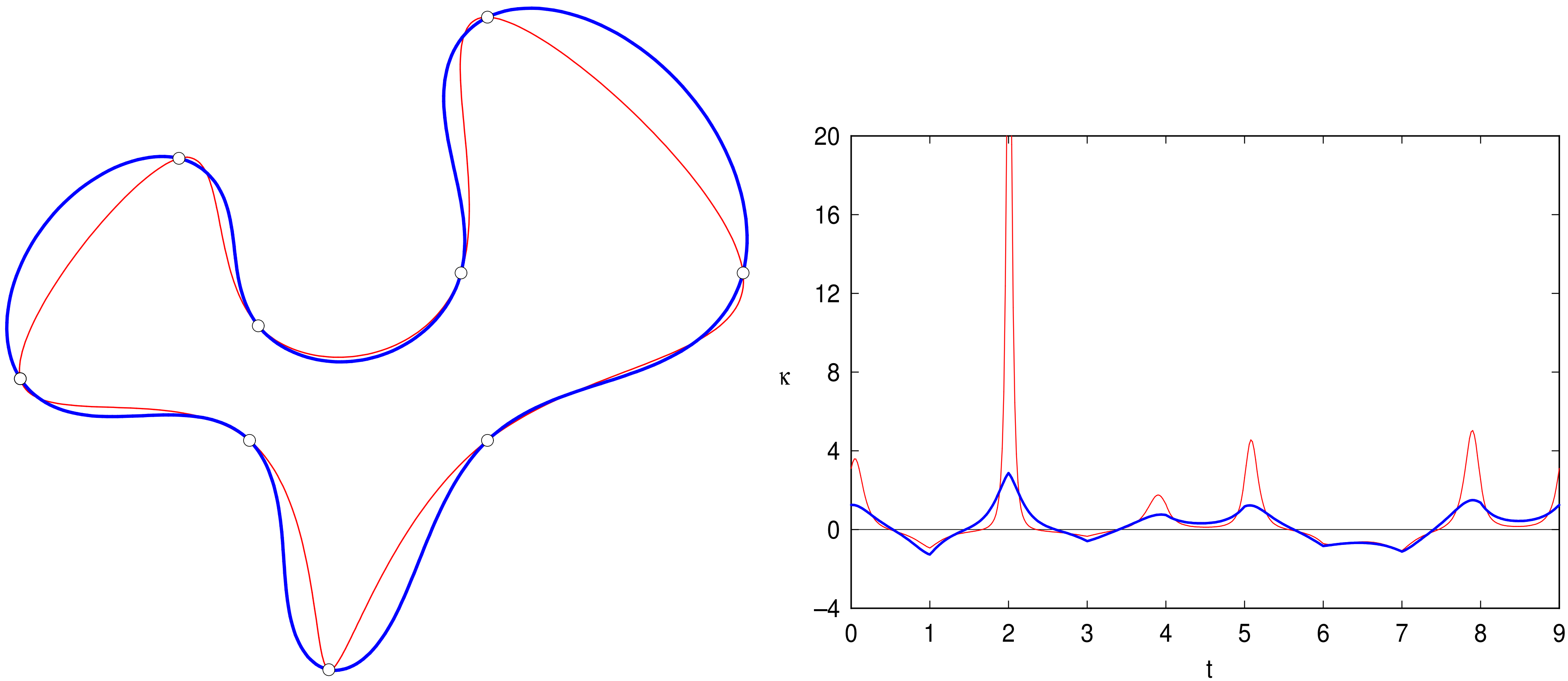

blue $=$ C^2 PH quintic spline, red $=$ “ordinary” C^2 cubic spline

solution method #2 — Newton-Raphson iteration

R. T. Farouki, B. K. Kuspa, C. Manni, and A. Sestini, Efficient solution of the complex quadratic tridiagonal system for C^2 PH quintic splines, *Numerical Algorithms* **27**, 35–60 (2001)

in applications, we want to compute only the “good” PH quintic spline

apply Newton-Raphson iteration to system $\mathbf{f}_i(\mathbf{z}_1, \ldots, \mathbf{z}_N) = 0\,,\ 1 \le i \le N$

recall that Jacobian matrix $\mathbf{M}_{ij} = \dfrac{\partial\,\mathbf{f}_i}{\partial\,\mathbf{z}_j}\,, \quad 1 \le i, j \le N$ is tridiagonal

in rows $i = 2, \ldots, N-1$, the only non–zero elements are

$$
\begin{aligned}
\mathbf{M}_{i,i-1} &= 6\,\mathbf{z}_{i-1} + 13\,\mathbf{z}_i + \mathbf{z}_{i+1}\,, \\
\mathbf{M}_{ii} &= 13\,\mathbf{z}_{i-1} + 54\,\mathbf{z}_i + 13\,\mathbf{z}_{i+1}\,, \\
\mathbf{M}_{i,i+1} &= \mathbf{z}_{i-1} + 13\,\mathbf{z}_i + 6\,\mathbf{z}_{i+1}\,.
\end{aligned}
$$

rows $i = 1$ and $i = N$ are modified to reflect the chosen end conditions writing $\mathbf{z} = (\mathbf{z}_1, \ldots, \mathbf{z}_N)^T$ and $\mathbf{f} = (\mathbf{f}_1, \ldots, \mathbf{f}_N)^T$, the Newton–Raphson iterations may be expressed as

$$\mathbf{z}^{(r+1)} = \mathbf{z}^{(r)} + \delta\mathbf{z}^{(r)}, \quad r = 0, 1, 2, \ldots$$

where $\delta\mathbf{z}^{(r)} = (\delta\mathbf{z}_1^{(r)}, \ldots, \delta\mathbf{z}_N^{(r)})^T$ is the solution of the linear system

$$\mathbf{M}^{(r)}\,\delta\mathbf{z}^{(r)} = -\,\mathbf{f}^{(r)}.$$

superscripts on $\mathbf{M}$ and $\mathbf{f}$ indicate evaluation at $\mathbf{z}^{(r)} = (\mathbf{z}_0^{(r)}, \ldots, \mathbf{z}_N^{(r)})$.

key step: find “sufficiently close” initial approximation $\mathbf{z}^{(0)} = (\mathbf{z}_1^{(0)}, \ldots, \mathbf{z}_N^{(0)})$

Kantorovich theorem: guaranteed convergence under verifiable conditions

choice of starting approximation

critical to successful Kanotorovich test & rapid convergence of iterations

strategy: equate mid–point derivatives of PH quintic spline to (known) mid–point derivatives of "ordinary" cubic spline that interpolates the same data points $\mathbf{p}_0, \ldots, \mathbf{p}_N$

yields a tridiagonal linear system for starting values $\mathbf{z}_1, \ldots, \mathbf{z}_N$

$$\mathbf{z}_{i-1} + 6\mathbf{z}_i + \mathbf{z}_{i+1} = 4\sqrt{6\Delta\mathbf{p}_i - (\mathbf{d}_{i-1} + \mathbf{d}_i)}\,, \quad i = 1, \ldots, N$$

where $\mathbf{d}_0, \ldots, \mathbf{d}_N$ are the nodal derivatives of the "ordinary" cubic spline, and equations $i = 1$ and $i = N$ are adjusted for the chosen end conditions

strategy is nearly infallible for smoothly–varying data points $\mathbf{p}_0, \ldots, \mathbf{p}_N$

efficiency of Newton-Raphson method

tridiagonal equations for NR increments $\delta\mathbf{z}^{(r)}$ — $O(N)$ solution cost — and quadratic convergence of the NR iterations $\Longrightarrow$ extremely efficient construction of large–N PH quintic splines

shape	$N+1$	homotopy method	Newton–Raphson
kidney	10	8.09 sec	0.11 sec
squiggly	15	656.21 sec	0.12 sec
quirky	19	1128.97 sec	0.23 sec
big open	35	—	0.40 sec
big closed	38	—	0.43 sec

Timing comparisons for C^2 PH quintic spline test curves

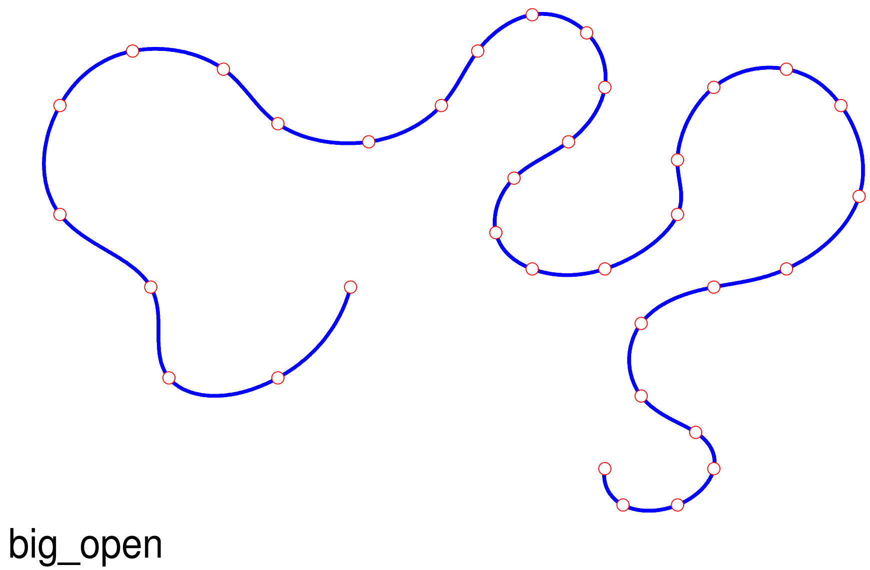

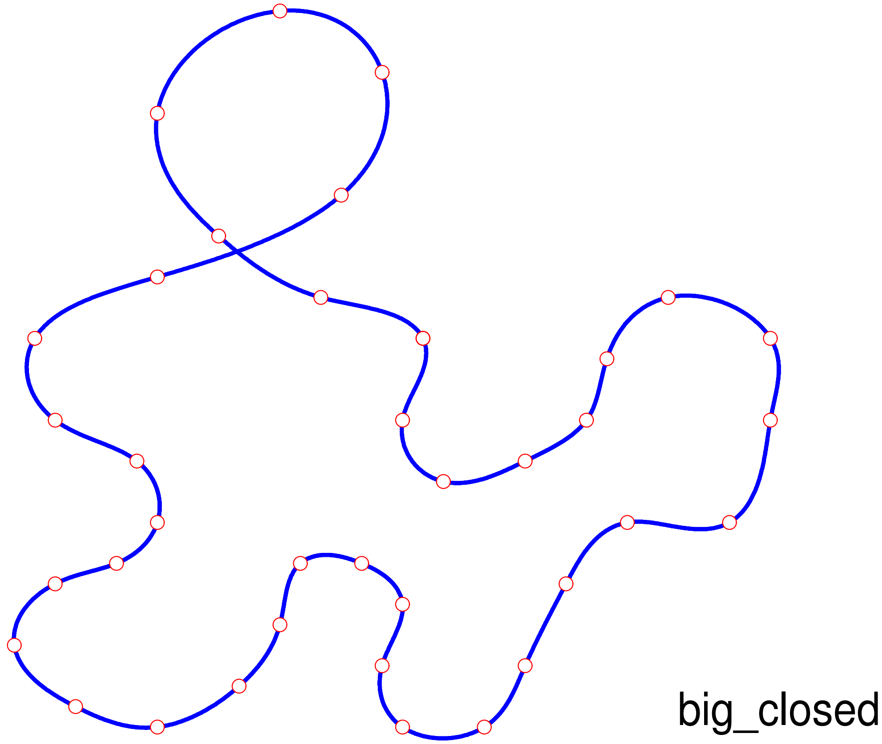

C^2 PH quintic splines computed by Newton–Raphson method for large N

design of C^2 PH splines by control polygons

F. Pelosi, M. L. Sampoli, R. T. Farouki, and C. Manni, A control polygon scheme for design of planar C^2 PH quintic spline curves, *Computer Aided Geometric Design* **24**, 28–52 (2007)

desire a control–polygon approach to constructing PH splines, that mimics the familiar and useful properties of cubic B–spline curves

non–linear nature of PH curves $\Longrightarrow$ there is no spline basis for them

strategy: control polygon defines a “hidden” interpolation problem for PH splines, to be solved by efficient Newton–Raphson method

C^2 PH quintic spline curve associated with a given control polygon and knot sequence is defined to be the “good” interpolant to the nodal points of the ordinary C^2 cubic spline curve with the same B–spline control points, knot sequence, and end conditions

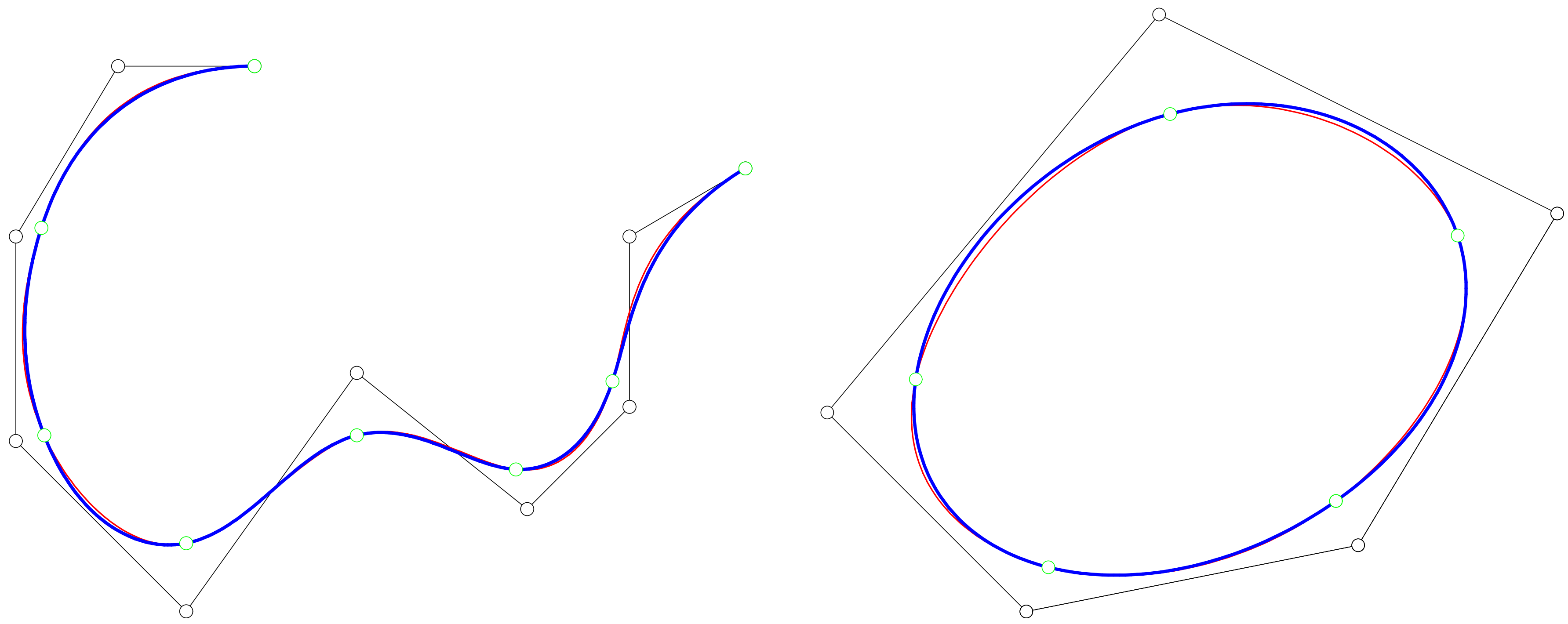

comparison of the “ordinary” cubic B–spline (red) and PH quintic spline (blue) curves defined by given control polygons and knot sequences

computation sufficiently fast for interactive modification of polygons

multiple knots may be introduced to reduce the continuity to C^1 or C^0

linear precision & local modification capability possible with double knots

. . . the three Russian brothers . . .

. . . Following the collapse of the former Soviet Union, the economy in Russia hit hard times, and jobs were difficult to find. Dmitry, Ivan, and Alexey — the Brothers Karamazov — therefore decided to seek their fortunes by emigrating to America, England, Australia . . .

Pythagorean quartuples of polynomials

$$x'^2(t) + y'^2(t) + z'^2(t) = \sigma^2(t) \qquad \Longleftrightarrow \qquad \begin{cases} x'(t) = u^2(t) + v^2(t) - p^2(t) - q^2(t) \\ y'(t) = 2\,[\,u(t)q(t) + v(t)p(t)\,] \\ z'(t) = 2\,[\,v(t)q(t) - u(t)p(t)\,] \\ \sigma(t) = u^2(t) + v^2(t) + p^2(t) + q^2(t) \end{cases}$$

R. Dietz, J. Hoschek, and B. Jüttler, An algebraic approach to curves and surfaces on the sphere and on other quadrics, *Computer Aided Geometric Design* **10**, 211–229 (1993)

R. T. Farouki and T. Sakkalis, Pythagorean–hodograph space curves, *Advances in Computational Mathematics*, **2** 41–66 (1994)

H. I. Choi, D. S. Lee, and H. P. Moon, Clifford algebra, spin representation, and rational parameterization of curves and surfaces, *Advances in Computational Mathematics* **17**, 5-48 (2002)

quaternion model for spatial PH curves

choose quaternion polynomial $\quad \mathcal{A}(t) \;=\; u(t) + v(t)\,\mathbf{i} + p(t)\,\mathbf{j} + q(t)\,\mathbf{k}$

$\rightarrow$ spatial Pythagorean hodograph $\quad \mathbf{r}'(t) \;=\; (x'(t), y'(t), z'(t)) \;=\; \mathcal{A}(t)\,\mathbf{i}\,\mathcal{A}^*(t)$

fundamentals of quaternion algebra

quaternions are four-dimensional numbers of the form

$$\mathcal{A} = a + a_x\,\mathbf{i} + a_y\,\mathbf{j} + a_z\,\mathbf{k} \qquad \text{and} \qquad \mathcal{B} = b + b_x\,\mathbf{i} + b_y\,\mathbf{j} + b_z\,\mathbf{k}$$

that obey the sum and (non-commutative) product rules

$$\mathcal{A} + \mathcal{B} = (a+b) + (a_x + b_x)\,\mathbf{i} + (a_y + b_y)\,\mathbf{j} + (a_z + b_z)\,\mathbf{k}$$

$$\begin{aligned} \mathcal{A}\,\mathcal{B} \;=\; & (ab - a_x b_x - a_y b_y - a_z b_z) \\ +\; & (a b_x + b a_x + a_y b_z - a_z b_y)\,\mathbf{i} \\ +\; & (a b_y + b a_y + a_z b_x - a_x b_z)\,\mathbf{j} \\ +\; & (a b_z + b a_z + a_x b_y - a_y b_x)\,\mathbf{k} \end{aligned}$$

basis elements 1, $\mathbf{i}$, $\mathbf{j}$, $\mathbf{k}$ satisfy $\mathbf{i}^2 = \mathbf{j}^2 = \mathbf{k}^2 = \mathbf{i}\,\mathbf{j}\,\mathbf{k} = -1$

equivalently, $\mathbf{i}\,\mathbf{j} = -\mathbf{j}\,\mathbf{i} = \mathbf{k}\,, \quad \mathbf{j}\,\mathbf{k} = -\mathbf{k}\,\mathbf{j} = \mathbf{i}\,, \quad \mathbf{k}\,\mathbf{i} = -\mathbf{i}\,\mathbf{k} = \mathbf{j}$

scalar-vector form of quaternions

set $\mathcal{A} = (a, \mathbf{a})$ and $\mathcal{B} = (b, \mathbf{b})$ — a, b and $\mathbf{a}$, $\mathbf{b}$ are scalar and vector parts

(a, b and $\mathbf{a}, \mathbf{b}$ also called the real and imaginary parts of $\mathcal{A}, \mathcal{B}$)

$$\mathcal{A} + \mathcal{B} = (a + b, \mathbf{a} + \mathbf{b})$$

$$\mathcal{A}\mathcal{B} = (ab - \mathbf{a} \cdot \mathbf{b}, a\,\mathbf{b} + b\,\mathbf{a} + \mathbf{a} \times \mathbf{b})$$

(historical note: Hamilton's quaternions preceded, but were eventually supplanted by, the 3-dimensional vector analysis of Gibbs and Heaviside)

$\mathcal{A}^* = (a, -\mathbf{a})$ is the conjugate of $\mathcal{A}$

modulus : $\quad |\mathcal{A}|^2 = \mathcal{A}^*\mathcal{A} = \mathcal{A}\mathcal{A}^* = a^2 + |\mathbf{a}|^2$

note that $\quad |\mathcal{A}\mathcal{B}| = |\mathcal{A}|\,|\mathcal{B}| \quad$ and $\quad (\mathcal{A}\mathcal{B})^* = \mathcal{B}^*\mathcal{A}^*$

unit quaternions & spatial rotations

any unit quaternion has the form $\mathcal{U} = (\cos\frac{1}{2}\theta, \sin\frac{1}{2}\theta\,\mathbf{n})$

describes a spatial rotation by angle θ about unit vector $\mathbf{n}$

for any vector $\mathbf{v}$ the quaternion product

$$\boxed{\tilde{\mathbf{v}} = \mathcal{U}\,\mathbf{v}\,\mathcal{U}^*}$$

yields the vector $\tilde{\mathbf{v}}$ corresponding to a rotation of $\mathbf{v}$ by θ about $\mathbf{n}$

here $\mathbf{v}$ is short-hand for a "pure vector" quaternion $\mathcal{V} = (0, \mathbf{v})$

unit quaternions $\mathcal{U}$ form a (non-commutative) group under multiplication

quaternion model for spatial PH curves

quaternion polynomial $\mathcal{A}(t) = u(t) + v(t)\,\mathbf{i} + p(t)\,\mathbf{j} + q(t)\,\mathbf{k}$

$$\text{maps to} \quad \mathbf{r}'(t) \;=\; \mathcal{A}(t)\,\mathbf{i}\,\mathcal{A}^*(t) \;=\; [\,u^2(t) + v^2(t) - p^2(t) - q^2(t)\,]\,\mathbf{i} \\ +\; 2\,[\,u(t)q(t) + v(t)p(t)\,]\,\mathbf{j} \;+\; 2\,[\,v(t)q(t) - u(t)p(t)\,]\,\mathbf{k}$$

rotation invariance of spatial PH form: rotate by θ about $\mathbf{n} = (n_x, n_y, n_z)$

define $\mathcal{U} = (\cos\frac{1}{2}\theta, \sin\frac{1}{2}\theta\,\mathbf{n})$ — then $\mathbf{r}'(t) \;\rightarrow\; \tilde{\mathbf{r}}'(t) = \tilde{\mathcal{A}}(t)\,\mathbf{i}\,\tilde{\mathcal{A}}^*(t)$

where $\tilde{\mathcal{A}}(t) \;=\; \mathcal{U}\,\mathcal{A}(t)$ (can interpret as rotation in $\mathbb{R}^4$)

solution of “fundamental” quaternion equation

for any given vector $\mathbf{v}$, find quaternions $\mathcal{A}$ satisfying $\mathcal{A}\,\mathbf{i}\,\mathcal{A}^* = \mathbf{v}$

such quaternions $\mathcal{A}$ map the unit vector $\mathbf{i}$ onto the given vector $\mathbf{v}$
by means of a scaling–rotation transformation

write $\hat{\mathbf{v}} = \dfrac{\mathbf{v}}{|\mathbf{v}|} = (\lambda, \mu, \nu)$ — obtain one–parameter family of solutions

$$\mathcal{A} = \sqrt{\frac{(1+\lambda)|\mathbf{v}|}{2}}\left(-\sin\phi + \cos\phi\,\mathbf{i} + \frac{\mu\cos\phi + \nu\sin\phi}{1+\lambda}\mathbf{j} + \frac{\nu\cos\phi - \mu\sin\phi}{1+\lambda}\mathbf{k}\right)$$

where ϕ = free angular variable

more compact from — $\mathcal{A} = \sqrt{|\mathbf{v}|}\,\mathbf{n}\,\exp(\phi\,\mathbf{i})$

where $\exp(\phi\,\mathbf{i}) = \cos\phi + \sin\phi\,\mathbf{i}$ and $\mathbf{n} = \dfrac{\mathbf{i}+\hat{\mathbf{v}}}{|\,\mathbf{i}+\hat{\mathbf{v}}\,|}$ = bisector of $\mathbf{i}$, $\hat{\mathbf{v}}$

spatial PH quintic Hermite interpolants

spatial PH quintic interpolating end points $\mathbf{p}_i$, $\mathbf{p}_f$ & derivatives $\mathbf{d}_i$, $\mathbf{d}_f$

$$\mathbf{r}'(t) \,=\, \mathcal{A}(t)\,\mathbf{i}\,\mathcal{A}^*(t)\,, \quad \mathcal{A}(t) \,=\, \mathcal{A}_0(1-t)^2 \,+\, \mathcal{A}_1 2(1-t)t \,+\, \mathcal{A}_2 t^2$$

$\rightarrow$ three equations in three quaternion unknowns $\mathcal{A}_0$, $\mathcal{A}_1$, $\mathcal{A}_2$

$$\mathbf{r}'(0) \,=\, \mathcal{A}_0\,\mathbf{i}\,\mathcal{A}_0^* \,=\, \mathbf{d}_i \qquad \text{and} \qquad \mathbf{r}'(1) \,=\, \mathcal{A}_2\,\mathbf{i}\,\mathcal{A}_2^* \,=\, \mathbf{d}_f$$

$$\begin{aligned} \int_0^1 \mathcal{A}(t)\,\mathbf{i}\,\mathcal{A}^*(t)\,\mathrm{d}t \;&=\; \tfrac{1}{5}\,\mathcal{A}_0\,\mathbf{i}\,\mathcal{A}_0^* \,+\, \tfrac{1}{10}(\mathcal{A}_0\,\mathbf{i}\,\mathcal{A}_1^* + \mathcal{A}_1\,\mathbf{i}\,\mathcal{A}_0^*) \\ &+\; \tfrac{1}{30}(\mathcal{A}_0\,\mathbf{i}\,\mathcal{A}_2^* + 4\,\mathcal{A}_1\,\mathbf{i}\,\mathcal{A}_1^* + \mathcal{A}_2\,\mathbf{i}\,\mathcal{A}_0^*) \\ &+\; \tfrac{1}{10}(\mathcal{A}_1\,\mathbf{i}\,\mathcal{A}_2^* + \mathcal{A}_2\,\mathbf{i}\,\mathcal{A}_1^*) \,+\, \tfrac{1}{5}\,\mathcal{A}_2\,\mathbf{i}\,\mathcal{A}_2^* \,=\, \mathbf{p}_f - \mathbf{p}_i \end{aligned}$$

- two–parameter family of solutions for given data $\mathbf{p}_i$, $\mathbf{p}_f$ and $\mathbf{d}_i$, $\mathbf{d}_f$
  3 variables ϕ_0, ϕ_1, ϕ_2 but interpolants depend only on differences

examples of spatial PH quintic Hermite interpolants

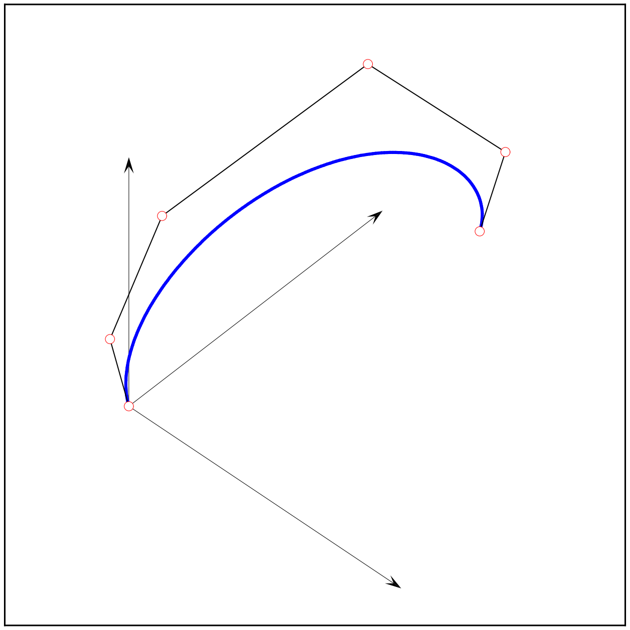

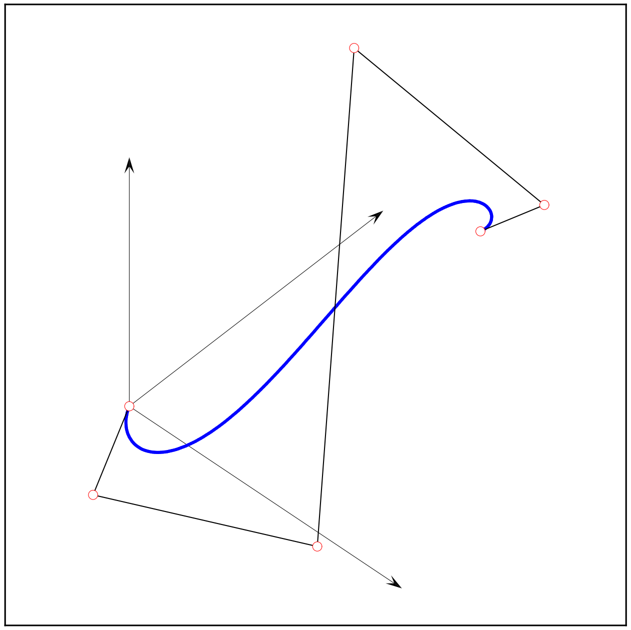

$\mathbf{p}_i = (0,0,0)$ and $\mathbf{p}_f = (1,1,1)$ for both curves

$\mathbf{d}_i = (-0.8, 0.3, 1.2)$ and $\mathbf{d}_f = (0.5, -1.3, -1.0)$ for curve on left,

$\mathbf{d}_i = (0.4, -1.5, -1.2)$ and $\mathbf{d}_f = (-1.2, -0.6, -1.2)$ for curve on right

choosing free parameters ϕ_0, ϕ_2 (set $\phi_1 = 0$ w.l.o.g.)

R. T. Farouki, C. Giannelli, C. Manni, and A. Sestini, Identification of spatial PH quintic Hermite interpolants with near–optimal shape measures, *Computer Aided Geometric Deisgn* **25**, 274–297 (2008)

total arc length depends only on difference $\phi_2 - \phi_0$ of two parameters

$\Rightarrow$ one–parameter family of Hermite interpolants with identical arc lengths

the Hermite interpolants of extremal arc length are helical PH curves

minimization of elastic energy $E = \int \kappa^2 \, \mathrm{d}s$ (computation intensive)

several efficient empirical measures for determining “optimal” ϕ_0, ϕ_2

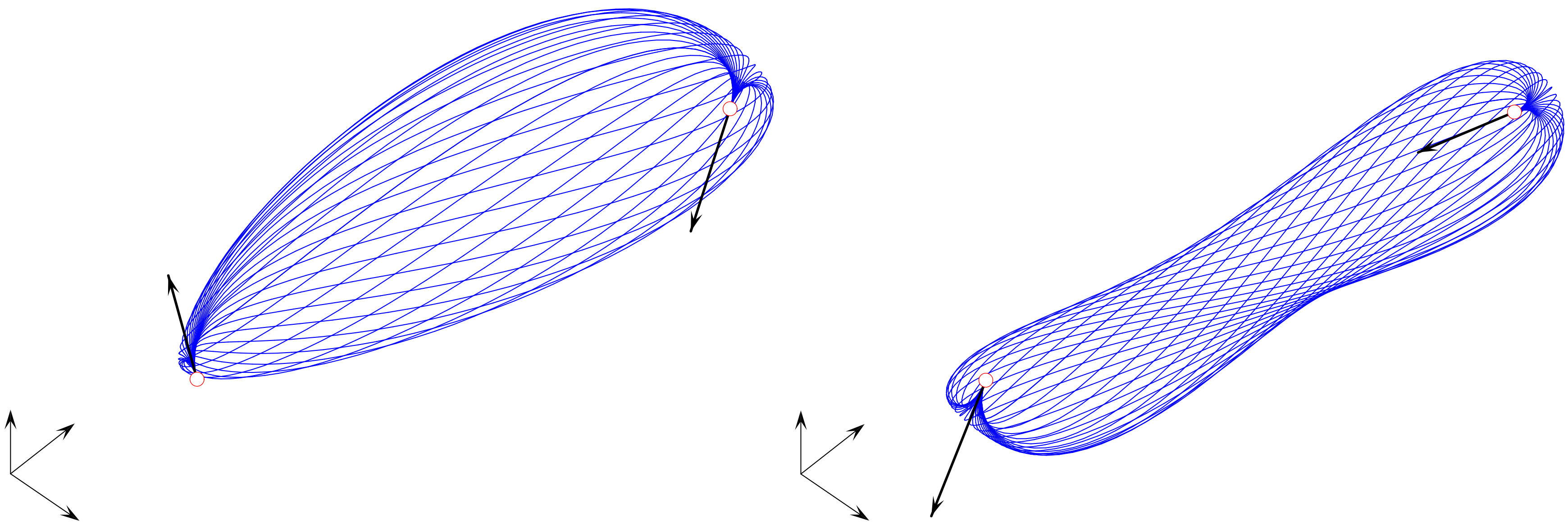

One–parameter families of spatial PH quintic interpolants, of identical arc length, defined by keeping $\phi_2 - \phi_0$ constant, and varying only $\frac{1}{2}(\phi_0 + \phi_2)$

taxonomy of "special spatial" PH curves

helical polynomial space curves

curve tangent $\mathbf{t}$ makes a constant angle α with a fixed unit vector $\mathbf{a}$ — i.e., $\mathbf{a} \cdot \mathbf{t} = \cos\alpha$ ($\mathbf{a} =$ axis of helix, $\alpha =$ pitch angle)

equivalently, curve has constant curvature–torsion ratio: $\kappa/\tau = \tan\alpha$

all helical polynomial curves are PH curves (implied by $\mathbf{a} \cdot \mathbf{t} = \cos\alpha$)

all spatial PH cubics are helical, but not all PH curves of degree ≥ 5

"double" Pythagorean–hodograph (DPH) curves

components of both $\mathbf{r}'(t)$ & $\mathbf{r}'(t) \times \mathbf{r}''(t)$ satisfy Pythagorean conditions

DPH curves have rational Frenet frames $(\mathbf{t}, \mathbf{n}, \mathbf{b})$ and curvatures κ

all helical polynomial curves must be DPH — not just PH — curves

all DPH quintics are helical, but not all DPH curves of degree ≥ 7

rational rotation–minimizing frame (RRMF) curves

rational adapted frames $(\mathbf{t},\mathbf{u},\mathbf{v})$ with angular velocity satisfying $\boldsymbol{\omega}\cdot\mathbf{t}\equiv 0$

RRMF curves are of minimum degree 5 (proper subset of PH quintics)

identifiable by quadratic (vector) constraint on quaternion coefficients

useful in spatial motion planning and rigid–body orientation control

construction through geometric Hermite interpolation algorithm

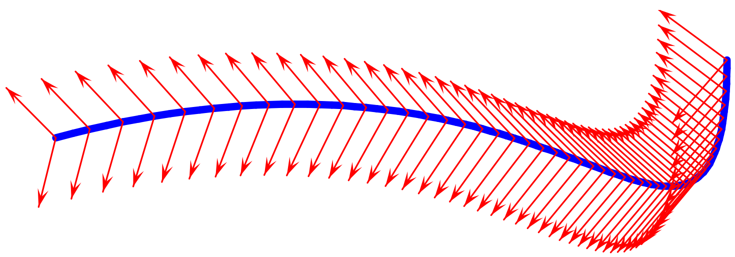

RMF

Frenet

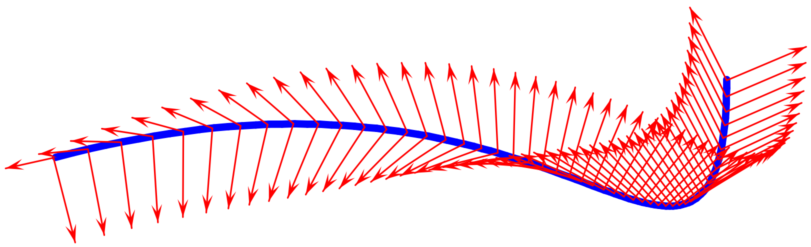

rational rotation-minimizing rigid body motions

R. T. Farouki, C. Giannelli, C. Manni, A. Sestini (2010), Design of rational rotation–minimizing rigid body motions by Hermite interpolation, *Math. Comp.*, submitted

- interpolate end points $\mathbf{p}_i$, $\mathbf{p}_f$ and frames $(\mathbf{t}_i, \mathbf{u}_i, \mathbf{v}_i)$ and $(\mathbf{t}_f, \mathbf{u}_f, \mathbf{v}_f)$ by PH quintic $\mathbf{r}(\xi)$ with rational rotation-minimizing frame $(\mathbf{t}(\xi), \mathbf{u}(\xi), \mathbf{v}(\xi))$

- RRMF condition for spatial PH quintics: $\mathcal{A}_1 \, \mathbf{i} \, \mathcal{A}_1^* = \mathcal{A}_0 \, \mathbf{i} \, \mathcal{A}_2^* + \mathcal{A}_2 \, \mathbf{i} \, \mathcal{A}_0^*$

- satisfying RRMF condition & end frame interpolation always possible — end point interpolation requires positive root of degree 6 equation

- diverse applications — to robotics, animation, spatial path planning, geometric sweeping operations, etc.

spatial C^2 PH quintic splines

- quaternion and Hopf map models for spatial C^2 PH quintic spline curves interpolating sequence of points $\mathbf{p}_0,\ldots,\mathbf{p}_N \in \mathbb{R}^3$ both incur one residual freedom per spline segment

- shape of spline interpolant sensitive to choice of free parameters

- early study — fix freedoms using “quaternion matching” condition

- optimize shape measure — e.g., proximity to a single PH cubic — to provide control-polygon-based design scheme

- specify arc lengths of spline segments as multiples of chord lengths, $\Delta s_k = \gamma_k \,|\,\mathbf{p}_k - \mathbf{p}_{k-1}|$ — for $\gamma_1 = \cdots = \gamma_N$ ($= \gamma$, say) we can use γ as a single tension parameter to alter interpolant shape

closure

- advantages of PH curves: rational offset curves, analytic real-time interpolators, exact bending energy, rotation-minimizing frames, etc.

- complex number and quaternion models are "natural" formulations for planar and spatial PH curves — rotation invariance, geometrical insight, simplified construction algorithms, etc.

- for planar PH curves, efficient & robust Hermite and spline interpolation algorithms are available for practical use

- for spatial PH curves, basic Hermite interpolation algorithm available with methods for "optimal" selection of two free parameters

- open problems for spatial PH curves — choice of multiple free parameters in C^2 spline formulation; geometric Hermite interpolation with RRMF curves; applications of rotation–minimizing frames in motion planning, animation, spatial orientation control, etc.